Bulletin of the Seismological Society of America, 90, 4, pp. 859–869, August 2000

Minimum Magnitude of Completeness in Earthquake Catalogs: Examples from Alaska, the Western United States, and Japan

by Stefan Wiemer and Max Wyss

Abstract We mapped the minimum magnitude of complete reporting, M_c, for Alaska, the western United States, and for the JUNEC earthquake catalog of Japan. M_c was estimated based on its departure from the linear frequency-magnitude relation of the 250 closest earthquakes to grid nodes, spaced 10 km apart. In all catalogs studied, M_c was strongly heterogeneous. In offshore areas the M_c was typically one unit of magnitude higher than onshore. On land also, M_c can vary by one order of magnitude over distance less than 50 km. We recommend that seismicity studies that depend on complete sets of small earthquakes should be limited to areas with similar M_c, or the minimum magnitude for the analysis has to be raised to the highest common value of M_c. We believe that the data quality, as reflected by the M_c level, should be used to define the spatial extent of seismicity studies where M_c plays a role. The method we use calculates the goodness of fit between a power law fit to the data and the observed frequency-magnitude distribution as a function of a lower cutoff of the magnitude data. M_c is defined as the magnitude at which 90% of the data can be modeled by a power law fit. M_c in the 1990s is approximately 1.2 ± 0.4 in most parts of California, 1.8 ± 0.4 in most of Alaska (Aleutians and Panhandle excluded), and at a higher level in the JUNEC catalog for Japan. Various sources, such as explosions and earthquake families beneath volcanoes, can lead to distributions that cannot be fit well by power laws. For the Hokkaido region we demonstrate how neglecting the spatial variability of M_c can lead to erroneous assumptions about deviations from self-similarity of earthquake scaling.

Introduction

The minimum magnitude of complete recording, M_c, is an important parameter for most studies related to seismicity. It is well known that M_c changes with time in most catalogs, usually decreasing, because the number of seismographs increases and the methods of analysis improve. However, differences of M_c as a function of space are generally ignored, although these, and the reasons for them, are just as obvious. For example, catalogs for offshore regions, as well as regions outside outer margins of the networks, are so radically different in their reporting of earthquakes that they should not be used in quantitative studies together with the catalogs for the central areas covered.

In seismicity studies, it is frequently necessary to use the maximum number of events available for high-quality results. This objective is undermined if one uses a single overall M_c cutoff that is high, in order to guarantee completeness. Here we show how a simple spatial mapping of the frequency-magnitude distribution (FMD) and application of a localized M_c cut-off can assist substantially in seismicity studies. We demonstrate the benefits of spatial mapping of M_c for a number of case studies at a variety of scales.

For investigations of seismic quiescence and the frequency-magnitude relationship, we routinely map the minimum magnitude of completeness to define an area of uniform reporting for study (Wyss and Martyrosian, 1998, Wyss *et al.,* 1999). Areas of inferior reporting (higher M_c), outside such a core area, are excluded because these data would contaminate the analysis. In seismicity studies where statistical considerations play a key role, it is important that results are not influenced by the choice of the data limits. If these limits are based on the catalog quality, then improved statistical robustness may be assured. For this reason we routinely map the quality of the catalog for selecting the data for our studies of seismic quiescence; however, homogeneity in M_c does not necessarily guarantee homogeneity in earthquake reporting, since changes in magnitude reporting influence the magnitude of homogeneous reporting (Habermann, 1986; Habermann, 1991; Zuniga and Wyss, 1995; Zuniga and Wiemer, 1999).

Our estimation of M_c is based on the assumption that, for a given, volume a simple power law can approximate the FMD. The FMD (Ishimoto and Iida, 1939; Gutenberg and

Richter, 1944) describes the relationship between the frequency of occurrence and magnitude of earthquakes:

$$\log_{10} N = a - bM, \quad (1)$$

where N is the cumulative number of earthquakes having magnitudes larger than M, and a and b are constants. Various methods have been suggested to measure b and its confidence limits (Aki, 1965; Utsu, 1965, 1992; Bender, 1983; Shi and Bolt, 1982; Frohlich and Davis, 1993). The FMD has been shown to be scale invariant down to a source length of about 10 m (Abercrombie and Brune, 1994) or approximately magnitude 0 event size. Some authors have suggested changes in scaling at the higher magnitude end (e.g., Lomnitz-Adler and Lomnitz 1979; Utsu, 1999) or for smaller events (Aki, 1987). However, neither of these suggested changes in slope will be relevant for the estimate of M_c because by far the dominant factor changing the slope of the FMD is incompleteness in reporting for smaller magnitudes. In Figure 1 we show the overall FMD in cumulative (Figure 1a) and noncumulative (Figure 1b) form for the three data sets we investigate. We assume that the drop in the number of events below M_c is caused by incomplete reporting of events.

Other studies that have addressed the completeness problem have either used changes between the day and nighttime sensitivity of networks (Rydelek and Sacks, 1989, 1992), comparison of amplitude-distance curves and the signal-to-noise ratio (Sereno and Bratt, 1989; Harvey and Hansen, 1994) or amplitude threshold studies (Gomberg, 1991) to estimate M_c. Waveform-based methods that require estimating the signal-to-noise ratio for numerous events at many stations are time-consuming and cannot generally be performed as part of a particular seismicity study. Using the FMD to estimate completeness is probably the simplest method. Our study demonstrates that despite some obvious shortcomings, spatially mapping of M_c based on the FMD is a quick yet useful tool for seismicity analysis and should in our opinion be a routine part of seismicity related studies.

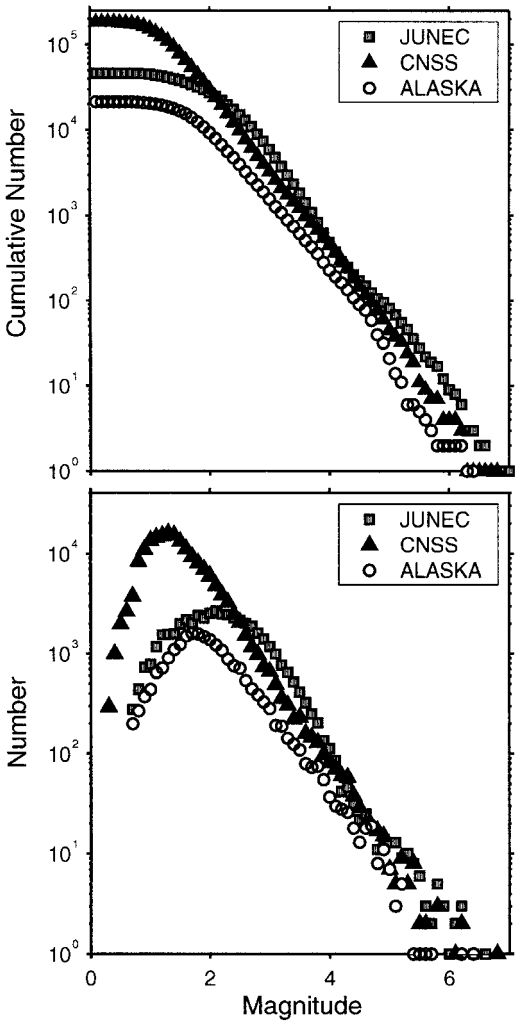

Figure 1. (a) Cumulative frequency-magnitude distribution of events for the three catalogs investigated. (b) Number of events in each magnitude bin for these catalogs.

Method

The first step toward understanding the characteristics of an earthquake catalog is to discover the starting time of the high-quality catalog most suitable for analysis. In addition, we seek to identify changes of reporting quality as a function of time. Issues connected with these problems are not the subjects of this article; they are dealt with elsewhere (Habermann, 1986; Habermann, 1991; Zuniga and Wiemer, 1999; Zuniga and Wyss, 1995). Here we assume that we know the starting date of the high-quality catalog, and that there are no changes of reporting (magnitude stretches and shifts) serious enough to corrupt the analysis we have in mind, so that we may proceed to map M_c.

Our estimate of M_c is based on the assumption of a Gutenberg-Richter (GR) power law distribution of magnitudes (equation 1). To evaluate the goodness of fit, we compute the difference between the observed FMD and a synthetic distribution. For incomplete data sets, a simple power law cannot adequately explain the observed FMD, so the difference will be high.

The following steps are taken to estimate M_c: First we estimate the b- and a-value of the GR law as a function of minimum magnitude, based on the events with $M \geq M_i$. We use a maximum likelihood estimate to estimate the b- and a-values and their confidence limits (Aki, 1965; Shi and Bolt, 1982; Bender, 1983). Next, we compute a synthetic distribution of magnitudes with the same b-, a- and M_i values, which represents a perfect fit to a power law. To estimate the goodness of the fit we compute the absolute difference, R, of the number of events in each magnitude bin between the observed and synthetic distribution

$$R(a, b, M_i) = 100 - \left(\frac{\sum_{M_i}^{M\max} |B_i - S_i|}{\sum_i B_i} 100 \right) \quad (2)$$

where B_i and S_i are the observed and predicted cumulative number of events in each magnitude bin. We divide by the total number of observed events to normalize the distribution. Our approach is illustrated in Figure 2, which shows R as function of M_i. If M_i is smaller then the 'correct' M_c, the synthetic distribution based on a simple power law (squares in Figure 2) cannot model the FMD adequately and, consequently, the goodness of fit, measured in percent of the total number of events, is poor. The goodness-of-fit value R increases with increasing M_i and reaches a maximum value of $R \sim 96\%$ at $M_c = 1.8$ in this example. At this M_c, a simple power law with the assumed b-, a-, and M_c value can explain 96% of the data variability. Beyond $M_i = 1.8$, R increases again gradually. In this study we map M_c at the 90% level, that is, we define M_c as the point at which a power law can model 90% or more of the FMD. For the example shown in Figure 2, we therefore define $M_c = 1.5$.

Not all FMDs will reach the 90% mark. In some cases the FMDs are too curved or bimodal to be fitted satisfactory by a simple power law. This can be due to strong spatial or temporal inhomogeneities in the particular sample, or actual physical processes within the earth. An example of the former would be a drastic change of the completeness of recording during the investigated period; an example of the latter might be a volcanic region where distinct earthquake families and swarms are frequent. It is important to identify these areas for studies of the FMD, because here a power law cannot be readily applied. Our method allows us to map the fit to a power law behavior at each node, based on the minimum value of R obtained.

For mapping M_c, we use the gridding technique applied in our studies of b-values and seismic quiescence (Wiemer and Wyss, 1997; Wiemer *et al.,* 1998; Wiemer and Katsumata, 1999). Grids with several thousand nodes spaced regularly at 1 to 20 km distances, depending on the size of the area to be covered, the density of earthquakes, and the computer power available, are arbitrarily placed over the study region, and we construct the FMD at each node for the N nearest events and estimate M_c using the approach outlined previously. At the same time, we compute a map of the goodness of fit to a power law by finding the minimum R from equation (2) at each node. The same type of spatial

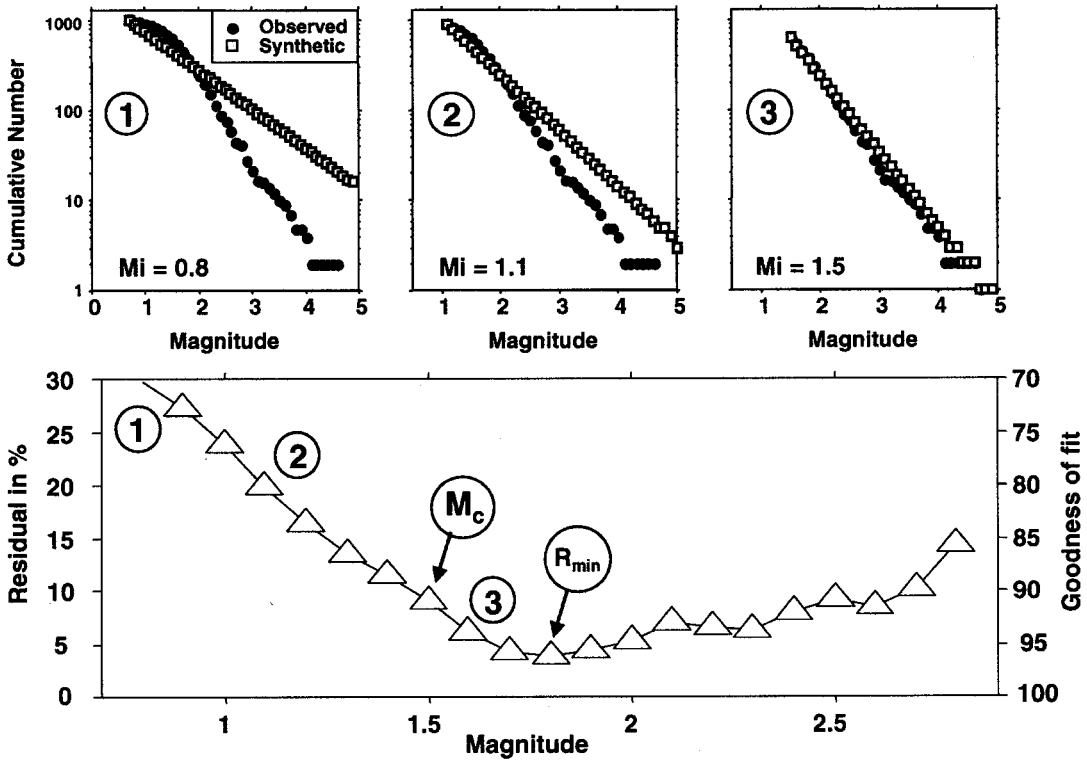

Figure 2. Explanation of the method by which we estimated the minimum magnitude of completeness, M_c. The three frames at the top show synthetic fits to the observed catalog for three different minimum magnitude cutoffs. The bottom frame shows the goodness of fit R, the difference between the observed and a synthetic FMD (equation 2), as a function of lower magnitude cut-off. Numbers correspond to the examples in the top row. The M_c selected is the magnitude at which 90% of the observed data are modeled by a straight line fit.

gridding can also be applied in cross sections (e.g., Wiemer and Benoit, 1996; Power *et al.,* 1998).

Data and Observations

In the following section, we apply the spatial mapping of M_c to three test cases: Alaska, Western United States, and Japan.

Alaska

The seismicity catalog compiled by the Alaska Earthquake Information Center (AEIC) for the period of January 1992–December 1998 contains a total of about 21,000 events for central and interior Alaska with a depth less than 60 km and $M > 0.5$. An epicenter map also identifying the main faults is shown in Figure 3c. We mapped M_c using a sample size of $N = 250$ and a node spacing of 10 km. The grid we created excludes low-seismicity areas. The sampling radii are typically $r = 70$ km, and none are larger than 200 km. M_c varies from values near 1.4 in the interior, near Fairbanks, and in the south, between Anchorage and Valdez (blue/purple in Figure 3a), to values of $M_c > 3$ offshore and on Kodiak island (red in Figure 3a). In Figure 4a we show a comparison of the FMDs for three areas: The vicinity of Fairbanks (M_c ~1.4), the Mt. McKinley area (M_c ~ 2.1), and Kodiak Island (M_c ~ 3.3).

A map of the goodness of fit to a GR distribution is shown in Figure 3b. Mapped is the parameter R; low R-values ($R < 90\%$), shown in hot colors indicate that only a poor fit to a GR distribution could be obtained. Several areas can be identified where the best fitting GR explains less than 90% of the observed distribution. The poorest fit to a GR

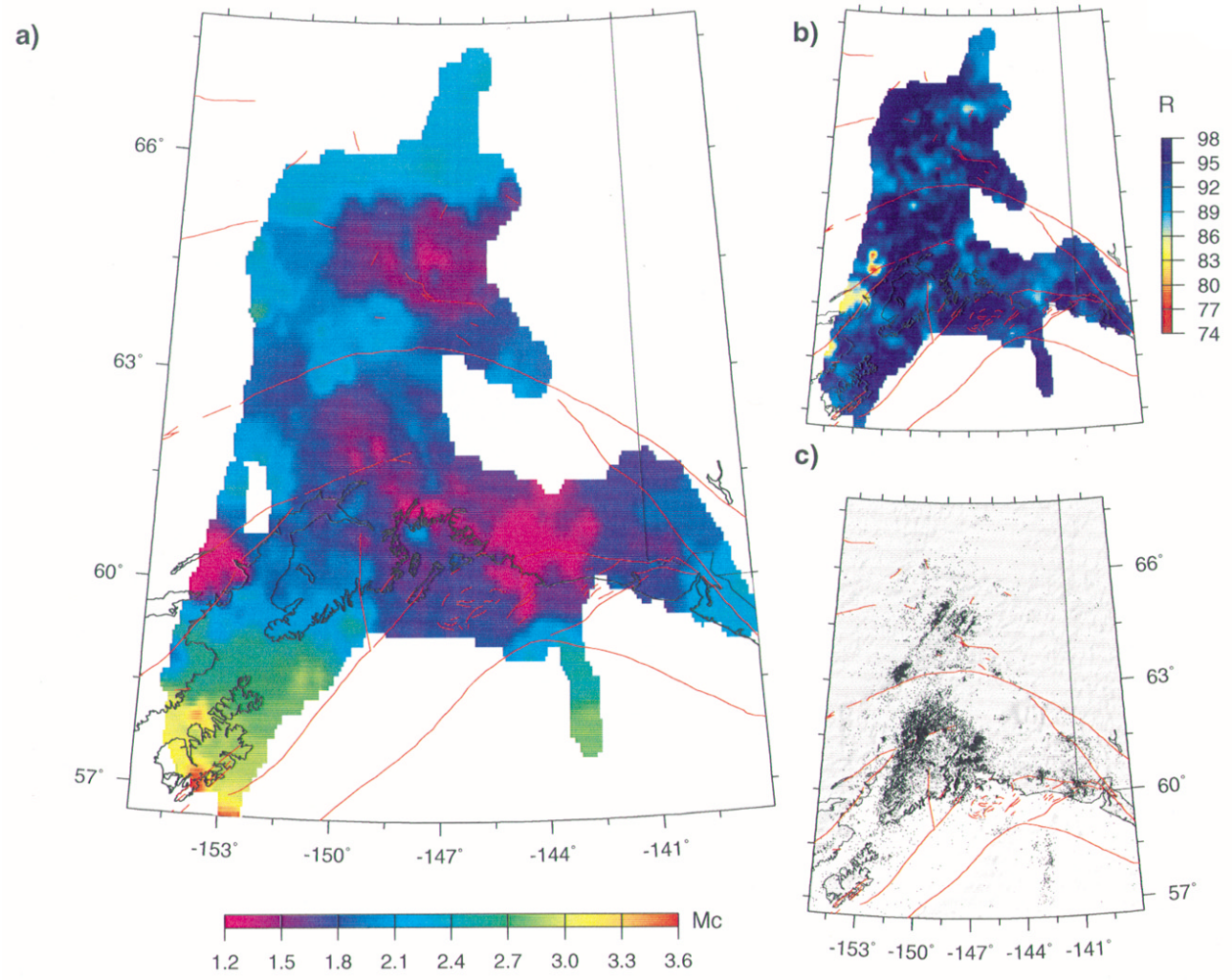

Figure 3. (a) Map of central and southern Alaska. Color-coded is the minimum magnitude of completeness, M_c, estimated from the nearest 250 earthquakes to nodes of a grid spaced 10 km apart. The typical sampling radii are $r = 75$ km, and all $r <$ 200 km. (b) Map of the local goodness of fit of a straight line to the observed frequency-magnitude relation as measured by the parameter R in percent of the data modeled correctly. (c) Epicenters of earthquakes in Central and Southern Alaska for the period 1992–1999 and depth $<$ 60 km. Major faults are marked by red lines.

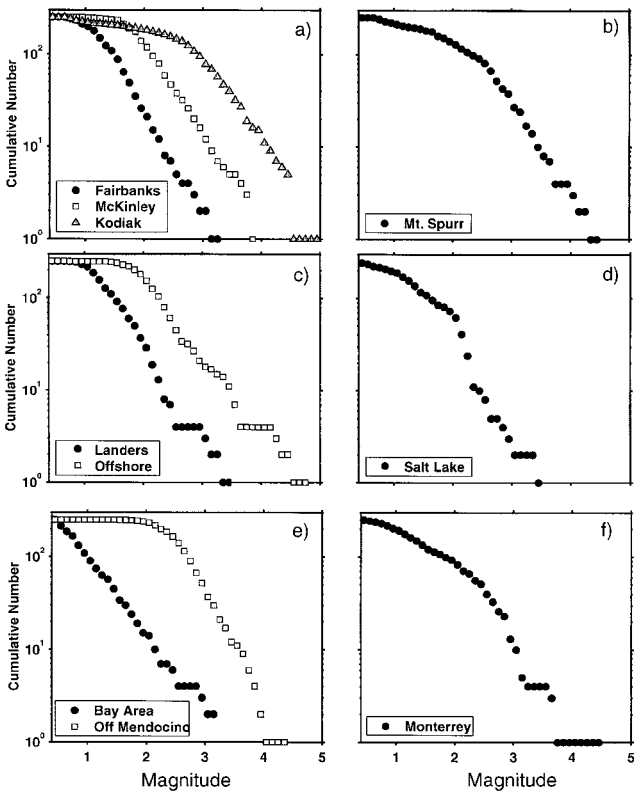

Figure 4. Frequency-magnitude distributions for selected areas. (a) Three areas in Alaska for which M_c ranges from 1.4 (Fairbanks) to 2.1 (McKinley) to 3.3 (Kodiak). (b) At volcanoes like Mt. Spurr, a bimodal distribution is often observed. In this case it is difficult to estimate M_c. (c) In Southern California, the offshore data ($M_c \geqq 2$) cannot be resolved to the same low-magnitude levels as on land, where $M_c \approx 1$ for many locations, such as near Landers. (d) An example of explosions, which, mixed into the earthquake catalog, can lead to unnatural FMDs. (e) In Northern California, some of the lowest $M_c \approx 0.4$ are observed in the San Francisco Bay area, and the highest values of $M_c > 2.5$ are observed far off Cape Mendocino. (f) An example of an FMD, which may be a hybrid of two populations because of a possible change of reporting rate as a function of time.

law ($R < 80\%$) can be observed near the volcanoes Mt. Spurr and Mt. Redoubt. In this area, the observed FMD (Figure 4b) is bimodal; two different populations of events are contained in the sample.

Western United States

We used the seismicity catalog compiled by the Council of the National Seismic Systems (CNSS) for the period of January 1995–May 1999 and events with a depths less than 30 km. Figure 5c shows the epicenter map of the area investigated. The spatial distribution of M_c is plotted in Figure 5a. The goodness-of-fit map (Figure 5b) indicates numerous small regions where the fit to GR is less than 90% satisfactory.

Southern California

Off-shore (Figures 4c and 5a) the resolution is not as good ($M_c \approx 2 \pm 0.2$) as it is on land and within the network, where $M_c < 1.7$ in most parts, except for the Mojave Desert (Figure 5a). The best resolution ($M_c \approx 0.8$) is achieved in the less populated Landers (Figures 4c and 5a), Salton Sea, San Jacinto, and Malibu areas. Pt. Conception, west of Santa Barbara, seems to be poorly covered ($M_c \approx 2.0$). In the Los Angeles area a resolution of $M_c \approx 1.5$ is achieved, which is remarkable, given the industrial noise level.

Northern California

The poorest coverage with $M_c > 2.7$ is seen far off the coast off Cape Mendocino (Figures 4e and 5a). At Cape Mendocino itself, $M_c \approx 2$. Most of the seismicity in the San Andreas fault system (west of the Great Valley) is resolved at levels of $M_c < 1.6$. The best job ($M_c \approx 0.8$) is achieved south of the San Francisco Bay to Parkfield (Figures 4e and 5a) and in the Mammoth Lake area. The border region with Nevada is not well covered; M_c rises above the 2.3 level in places. M_c also increases to $\sim$2 at the boundary between the northern and southern California seismic networks, south of Parkfield.

Japan

Our analysis is based on the Japan University Network (JUNEC) catalog for the period of January 1986–December 1990. Japan is covered by regional seismograph networks, which are run separately by universities and government research laboratories. JUNEC combined these data in a single catalog. The epicenter map for earthquakes with depths shallower than 35 km is shown in Figure 6c, the spatial distribution of M_c is imaged in Figure 6a. The M_c in the subducting slab beneath central Japan is shown in Figure 7.

In this catalog the seismicity located farther than about 100 km offshore is resolved only above the $M_c \approx 3.2$ level (Figure 6a). Within approximately 100 km from the coast, the completeness magnitude varies between 2.5 and 2.8. The areas in central Japan, near Tokyo and near Kyoto show the lowest M_c of about 1.3, whereas in northern Japan, $M_c \approx 2.4$ in this catalog.

The cross-sectional analysis in the Kanto region, central Japan (Figure 7) reveals the lowest M_c level ($M_c \approx 2.$) onshore. With increasing distance from land, M_c increases gradually to values greater than 3. Deep earthquakes in the subducting plate show a $M_c \approx 3$ at 200 km depth, and $M_c \approx 3.5$ at 400-km depth.

This analysis does not represent the full extent of information available on seismicity in Japan. The catalogs of individual organizations such as Bosai and Tohoku University, for example, resolve the areas covered by their networks to significantly lower magnitudes than the JUNEC catalog does. However, since the JUNEC catalog is readily available, and because it covers all of Japan, the variations of M_c in it are of interest.

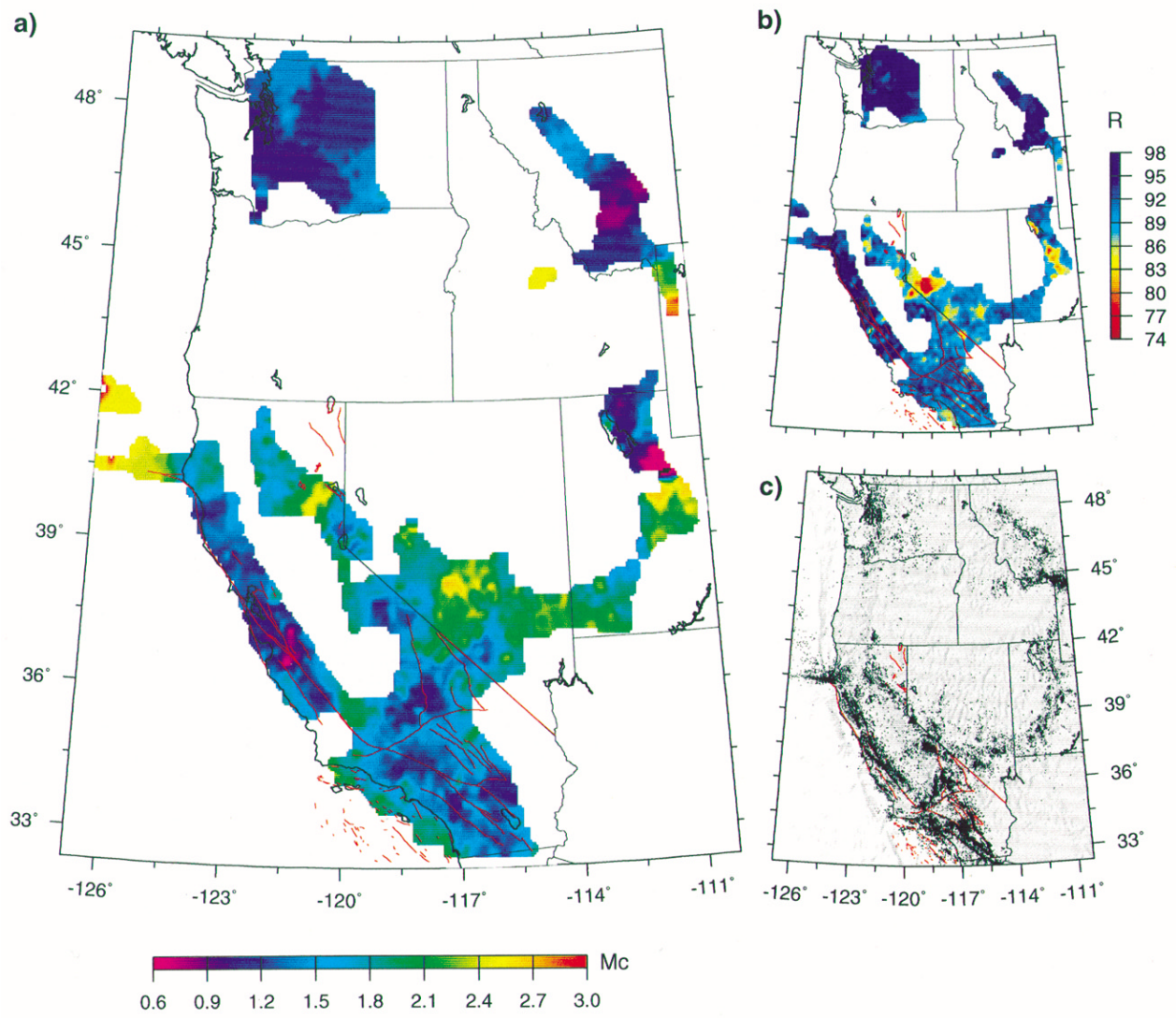

Figure 5. (a) Map of the western United States. Color-coded is the minimum magnitude of completeness, M_c estimated from the nearest 250 earthquakes to nodes of a grid spaced 10 km apart. The typical sampling radii are $r = 50$ km, and all $r < 150$ km. (b) Map of the local goodness of fit of a straight line to the observed frequency-magnitude relation as measured by the parameter R in percent of the data modeled correctly. (c) Epicenters of earthquakes in the western United States for the period 1993–1998 and depth < 30 km. Red lines mark major faults in California.

Discussion and Conclusions

Spatially Mapping M_c

The magnitude of completeness varies spatially throughout all seismic networks. By assessing the goodness of fit to a power law, we can reliably and quickly map out the spatial variability of M_c, based purely on catalog data. A solid knowledge of M_c is important for many seismicity and probabilistic earthquake hazard studies, and we propose that spatially mapping M_c should be performed routinely as part of seismicity studies. (The software used in this study can be freely downloaded as part of the ZMAP seismicity analysis package; *http://www.seismo.ethz.ch/staff/stefan*). Knowing the spatial distribution of M_c is important for regional studies that use bulk b-values. By excluding high M_c areas, the magnitude threshold for analysis can be lowered and the amount of data available for analysis increased. For studies that address the spatial variability of the FMD, knowledge of the spatial distribution of M_c is imperative.

From the M_c maps (Figures 3, 5, and 6) we see that in most of Alaska the seismicity is resolved to $M_c = 1.8 \pm 0.4$, in most of California the completeness level is at $M_c + 1.2 \pm 0.4$, and in the JUNEC catalog of Japan it is not better than in Alaska. In the Aleutian islands of Alaska, the seis-

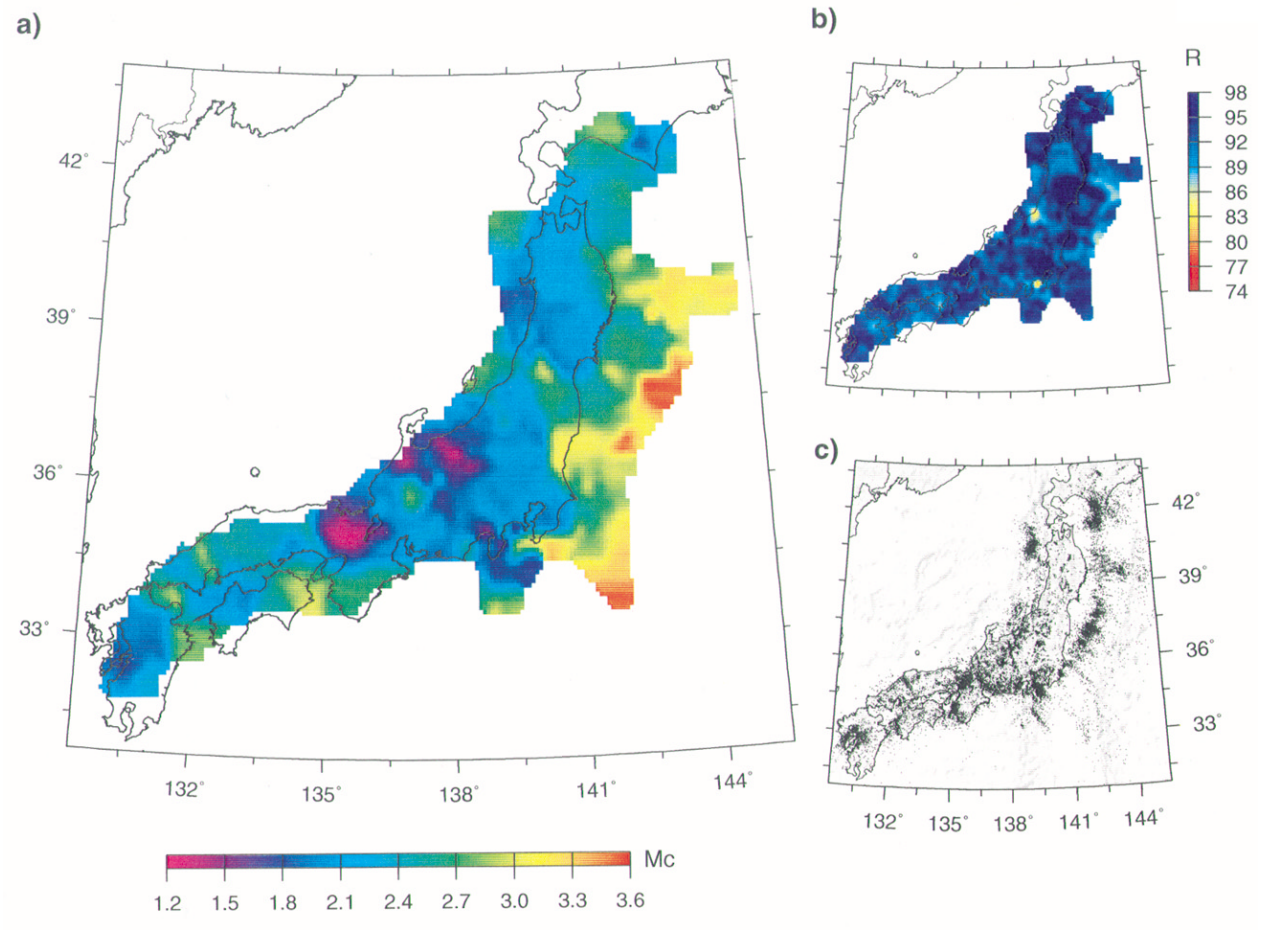

Figure 6. (a) Map of Japan. Color-coded is the minimum magnitude of completeness, M_c estimated from the nearest 250 earthquakes to nodes of a grid spaced 10 km apart. The typical sampling radii are $r = 62$ km, and all $r < 150$ km. (b) Map of the local goodness of fit of a straight line to the observed frequency-magnitude relation as measured by the parameter R in percent of the data modeled correctly. (c) Epicenters of earthquakes in Japan for the period 1986–1992 and depth < 35 km.

mically most active part of the United States, the M_c exceeds that of the SW corner of Kodiak island, where $M_c = 3.4$. For the CNSS catalog, event data are merged rather than the phase data, before relocation with the combined set. Thus events near network boundaries are detected and located from one network only. This is consistent with the increase in M_c we see near CNSS network boundaries (Fig. 5).

Heterogeneity of the M_c is considerable in some areas. M_c can change by one full magnitude unit over distances of less than 50 km. Some of these cases may be known to the network operators and determined to be acceptable; others may not be known and could possibly be reviewed. For example, it may not be desirable to have a relatively high M_c along the coast west of Santa Barbara, whereas an improvement of the resolution to lower M_c values may not be economical in some places, like western and central Alaska. Analysis of M_c as a function of space and time may help network operators to make decisions on an informed basis for improving their monitoring efforts.

At the levels of completeness seen in California, faults can be mapped quite well, as one can see in the epicenter maps of Figures 5c. However, at the somewhat higher levels of completeness in Alaska it becomes more difficult to map faults (Fig. 3a). In Japan the level of completeness shown by the JUNEC catalog is not considered adequate. Not only do regional networks furnish lower M_c values, but also Japan has undertaken a new, strong push to install many more seismographs to monitor the seismicity in much greater detail.

We investigated the correlation between the density of seismic stations and the magnitude of completeness. At each node of the M_c grid for California (Fig. 5) and Alaska (Fig. 3), we find the distance in kilometers of the 4th closest station to this node. Since four stations are the minimum number required to obtain a hypocenter solution, this distance is one possible measure of the local density of stations. For this simple approximation we only consider vertical channels. Results are shown in Figure 8a for California and 8b for Alaska. As expected, M_c increases systematically with in-

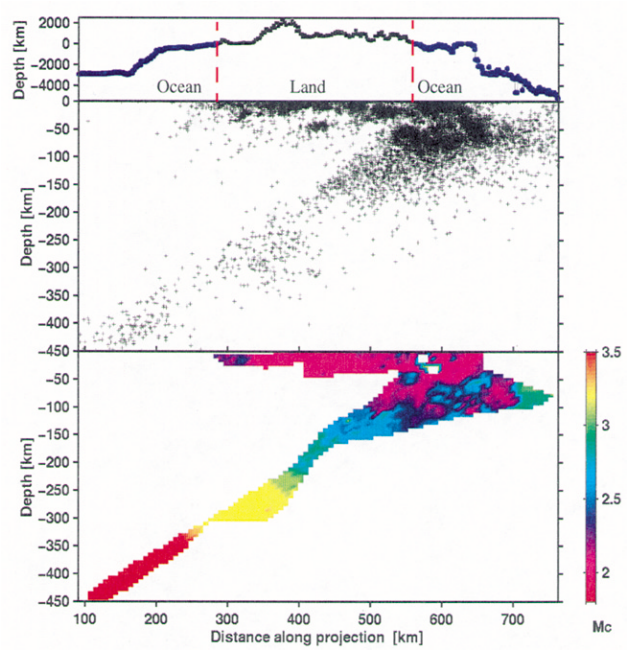

Figure 7. Cross-sectional view through the subducting Pacific plate in the Tohoku region, northern Japan. The top frame shows topography and bathymetry. The middle frame displays hypocenter location obtained from the JUNEC catalog for the period January 1986–December 1991. The bottom frame represents the distribution of M_c.

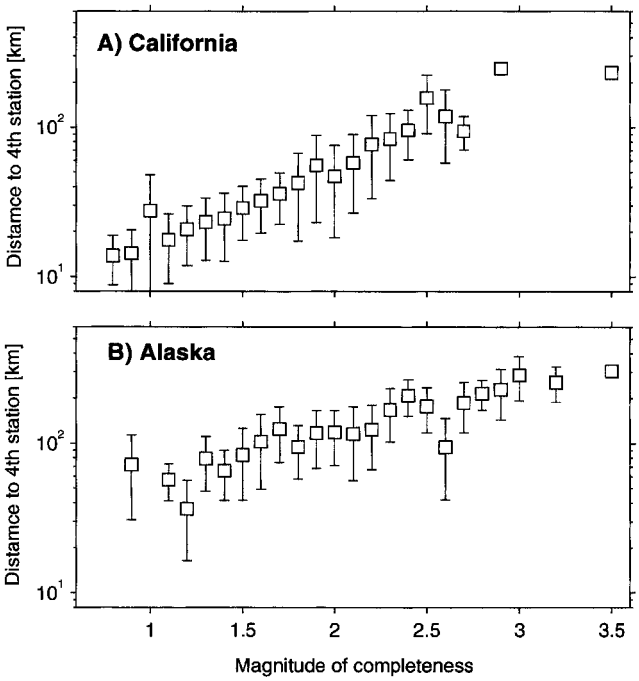

Figure 8. Plot of the distance to the 4th nearest station as a function of M_c. (Top) Based on the M_c map for California (Fig. 5). (Bottom) Based on the M_c map for Alaska (Fig. 3).

creasing distance; however, the data show considerable spread and outliers. The curve for Alaska is systematically higher than the one for California; particularly for small M_c. We speculate that factors beyond station density, such as the ambient noise level at the sites, influence M_c; in Alaska the ambient noise due to human activity is lower than in highly populated California. These plots (Figure 8) can give network operators a rough estimate what decrease in M_c might be possible through network densification.

In past studies (Wiemer and Katsumata, 1999; Wiemer and McNutt, 1997; Wyss *et al.,* 2000) we have estimated M_c using the point of maximum curvature of the FMD. This simpler measure delivers a good first estimate of M_c, however, it tends to underestimate M_c in the case of gradually curved FMDs that are indicative of spatial and temporal heterogeneity of earthquake catalogs. A test for the Alaska data set shows that, averaged over all nodes, the difference in M_c between the two methods is 0.13. However, differences at a few nodes can be as high as 0.5. We consider the presented measure of M_c to be superior because it also identifies volumes in which a power law distribution of events cannot be assumed and because it applies a more quantitative criterion. Tests performed on the diverse data sets presented here have confirmed that the method to estimate M_c introduced here is robust and reliable.

Estimating M_c solely based on the FMD has some obvious drawbacks. For example, M_c cannot be estimated in areas of low seismicity. Unlike methods based on the signal-to-noise ratio and amplitude-distance curves (Gomberg, 1991; Harvey and Hansen, 1994; Sereno and Bratt, 1989), our method cannot forecast the detection capability of a network, neither is it capable of forecasting M_c based on hypothetical network configurations. It does, however, result in a reliable first-order approximation of the capabilities of seismic networks in the areas most interest: high-seismicity areas. The advantage of our method is that it can be performed easily, without requiring a time-consuming study of signal-to-noise ratio and amplitude-distance curves. Therefore, it can be applied as a routine part of any seismicity-related study.

Estimating M_c based on the difference in day and nighttime sensitivity (Rydelek and Sacks, 1989, 1992) has the drawbacks that (1) large samplesizes are need to estimate M_c, thus seriously limiting the ability to spatially map M_c; (2) contamination through quarry blast exists; (3) the method cannot readily be applied in areas with low cultural noise, such as Alaska. However, unlike our approach, no assumption about the linearity of the FMD is made.

Non-Power Law Behavior

By assessing the goodness of fit to a power law, we can identify areas where the estimate of M_c is likely to be inaccurate (Figs. 3b, 5b, 6b), that is, where R $<$ 90%. These areas deserve special attention in hazard and seismicity-related studies, because here extrapolations to larger magnitudes that are commonly done in probabilistic hazard as-

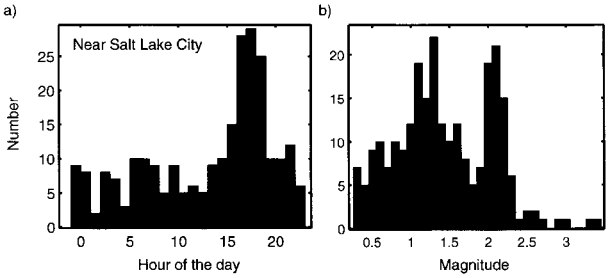

Figure 9. (a) Histogram of the hourly number of events south of Salt Lake City, Utah. The corresponding FMD is shown in Fig. 4d. The peak in the hourly distribution indicates that this region contains a large percentage of explosions, because many more events occur during the afternoon than at other times. (b) Histogram of the magnitudes for the same sample.

sessments must be considered less reliable. Volant and Scotti (1998) proposed to estimate the standard deviation of the *b*-value with a nonweighted least squares technique to quantify the departure from linearity in the tail of the FMD. Using this technique, they were able to map zones of nonlinear behavior in the Western Alps. It is not within this study to systematically investigate the cause of the non-power law behavior; however, for selected areas we demonstrate likely reasons.

The most outstanding non-power law curve in Alaska (Fig. 3a) is located near the volcanoes Mt. Spurr and Mt. Redoubt. Here, local dense networks are installed on the volcanoes, adding a population of small-magnitude events to the regional data set. This, and the possible inclusion of earthquake swarms and families common at volcanoes, result in a bimodal FMD as shown in Figure 4b that is the

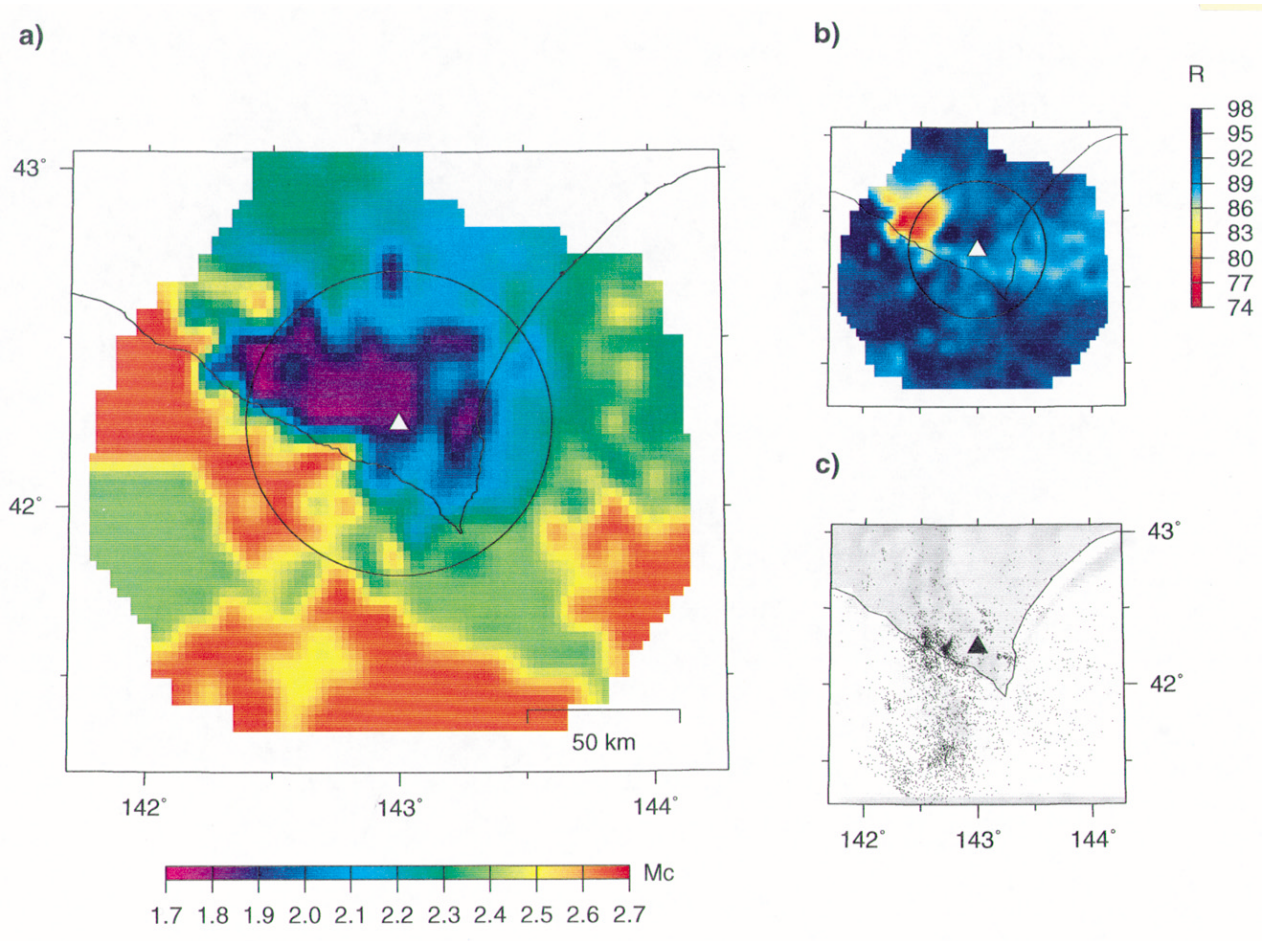

Figure 10. (a) Map of the southeastern tip of Hokkaido, Japan. Color-coded is the minimum magnitude of completeness, M_c, estimated from the nearest 250 earthquakes to nodes of a grid spaced 5 km apart. The triangle marks the location of station KMU; the circle indicates the volume analyzed by Rydelek and Sacks (1989) and Taylor *et al.* (1990). (b) Map of the local goodness of fit of a straight line to the observed frequency-magnitude relation as measured by the parameter R in percent of the data modeled correctly. (c) Epicenters of earthquakes for the period 1986–1992 and depth <45 km.

telltale sign of combining populations of events with different properties.

In Utah we find low *R*-values south of Salt Lake City (Fig. 5b), and the respective FMD is shown in Figure 4d. In this region, we also notice a strong gradient in the M_c values (Fig. 5a). In a plot of the hourly distribution of events for this volume (Fig. 9a), one notices a dominant peak during daytime hours, which is a telltale sign of blast activity (Wiemer and Baer, 2000). The combined FMD of the explosions that preferably scale around *M*2 (Fig. 9b) and natural earthquake results in a strongly nonlinear behavior of the FMD.

Rydelek and Sacks (1989) and Taylor *et al.* (1990) claim to have identified a deviation from the "common lore of linear *b*-values and the idea of the self similar earthquake process" when analyzing crustal and deep events for the period 1977–1986 with 50 km of the station KMU, Hokkaido, Japan (143.0 E, 42.25 N). However, when analyzing the spatial variability of M_c using the JUNEC catalog, based on the same network but for the period 1986–1992, we find a much simpler explanation of their observation: Within the sample volume ($R < 50$ km, depths < 45 km, black circle in Fig. 10a), M_c varies drastically between onshore ($M_c \sim 1.8$) and offshore ($M_c \sim 2.5$) volumes. When mixing these different populations in one bulk analysis, a biased, low estimate of M_c is obtained, leading to the erroneous claim that the FMD is not linear. To demonstrate this point, we plot in Figure 11 the FMD for the onshore (triangles) and offshore (squares) population, as well as the combined (circles) population. The offshore population clearly is not complete to values of $M_c \sim 1.8$ as assumed by Rydelek and Sacks (1989) and Taylor *et al.* (1990). Similar variability of M_c between the deep and shallow earthquakes analyzed by Taylor *et al.* (1990) can be demonstrated, suggesting that in this case also the heterogeneity of M_c caused the nonlinearity of the FMD.

We conclude that a careful estimate of the spatial and temporal homogeneity of M_c is needed before any claim of deviations from a power law behavior for small magnitudes can be made. The daytime to nighttime activity variation criteria applied in Rydelek and Sacks (1989) and Taylor *et al.* (1990) do not seem able to determine M_c correctly if M_c varies spatially. The fraction of events to the SW of station KMU that requires a $M_c > 2.5$ (Fig. 10) does not make itself known in the phasor plots used by Rydelek and Sacks (1989) and Taylor *et al.* (1990).

Based on the examples listed previously and others we studied, we conclude that most non-power law FMDs are caused by (1) artifacts in the catalog, for example, changes in M_c as a function of time; (2) mixing heterogeneous population of events, for example, explosions and tectonic earthquakes, or volcanic earthquake families and tectonic earthquakes; and (3) spatially heterogeneous M_c distribution. We suspect that, after eliminating these so-called contaminations, most earthquake populations can be adequately described by a power law for a wide range of magnitudes.

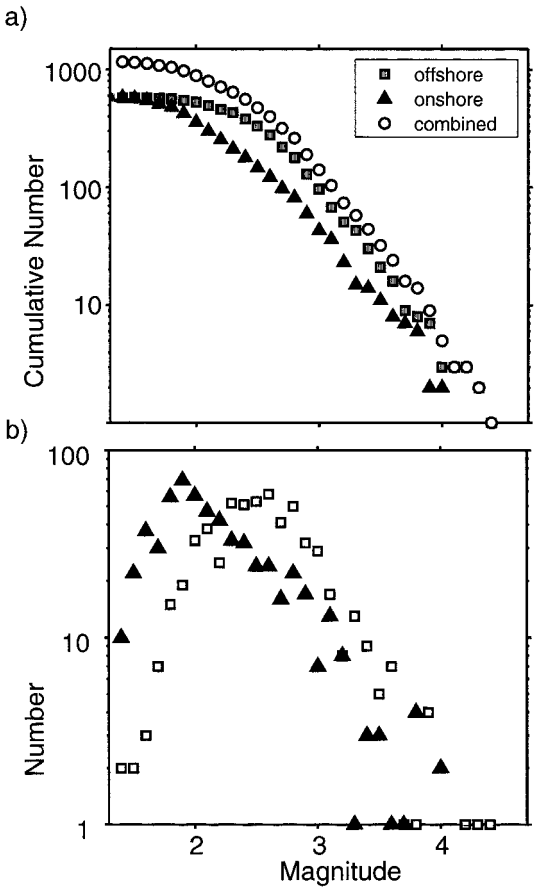

Figure 11. (a) Cumulative FMD of all earthquakes within 50 km of station KMU (Figure 9), compared to the FMDs of the separate onshore and offshore data sets. (b) Number of events in each magnitude bin. The offshore population of events is complete to M_c about 2.5–2.8, not $M_c = 1.8$ as concluded by Rydelek and Sacks (1989) and Taylor *et al.* (1990).

Acknowledgments

The authors would like to thank Walter Arabasz, Fred Klein, Andy Michael, Charlotte Rowe, Oona Scottie, Suzan van der Lee, Philippe Volant, and Ramon Zuniga for comments and suggestions that helped to improve the manuscript. Yuzo Toya helped to implement some of the software used in this study. Additional thanks to the organizations that made available their data for this study: The Alaska Earthquake Information Center and the NCEDC and its contributing institutions and the Japanese National University Earthquake Consortium for producing a national earthquake catalog. Support for this work has been provided by the Swiss Seismological Service and ETH, NSF grant EAR 9614783 and the Wadati endowment at the Geophysical Institute of the University of Alaska Fairbanks. This article is Contribution Number 1111 of the Geophysical Institute, ETHZ.

References

Abercrombie, R. E., and J. N. Brune (1994). Evidence for a constant b-value above magnitude 0 in the southern San Andreas, San Jacinto, and San Miguel fault zones and at the Long Valley caldera, California, *Geophys. Res. Lett.* **21,** no. 15, 1647–1650.

Aki, K. (1965). Maximum likelihood estimate of b in the formula log N = a − bM and its confidence limits, *Bull. Earthquake Res. Inst.* **43,** 237–239.

Aki, K. (1987). Magnitude frequency relation for small earthquakes: a clue to the origin of fmax of large earthquakes, *J. Geophys. Res.* **92,** 1349–1355.

Bender, B. (1983). Maximum likelihood estimation of b-values for magnitude grouped data, *Bull. Seism. Soc. Am.* **73,** 831–851.

Frohlich, C., and S. Davis (1993). Teleseismic b-values: or, much ado about 1.0, *J. Geophys. Res.* **98,** 631–644.

Gomberg, J. (1991). Seismicity and detection/location threshold in the southern Great Basin seismic network, *J. Geophys. Res.* **96,** no. B10, 16,401–16,414.

Gutenberg, R., and C. F. Richter (1944). Frequency of earthquakes in California, *Bull. Seism. Soc. Am.* **34,** 185–188.

Habermann, R. E. (1986). A test of two techniques for recognizing systematic errors in magnitude estimates using data from Parkfield, California, *Bull. Seism. Soc. Am.* **76,** 1660–1667.

Habermann, R. E. (1991). Seismicity rate variations and systematic changes in magnitudes in teleseismic catalogs, *Tectonophysics* **193,** 277–289.

Harvey, D., and R. Hansen (1994). Contributions of IRIS data to nuclear monitoring, *IRIS Newsletter* **13,** 1.

Ishimoto, M., and K. Iida (1939). Observations of earthquakes registered with the microseismograph constructed recently, *Bull. Earthquake Res. Inst.* **17,** 443–478.

Lomnitz-Adler, J., and C. Lomnitz (1979). A modified form of the Gutenberg-Richter magnitude-frequency relation, *Bull. Seism. Soc. Am.* **69,** 1209–1214.

Power, J. A., M. Wyss, and J. L. Latchman (1998). Spatial variations in frequency-magnitude distribution of earthquakes at Soufriere Hills volcano, Montserrat, West Indies, *Geophys. Res. Lett.* **25,** 3653–3656.

Rydelek, P. A., and I. S. Sacks (1989). Testing the completeness of earthquake catalogs and the hypothesis of self-similarity, *Nature* **337,** 251–253.

Rydelek, P. A., and I. S. Sacks (1992). Comment on "Seismicity and detection/location threshold in the southern Great Basin seismic network" by Joan Gomberg, *J. Geophys. Res.* **97,** no. B11, 15,361–15,362.

Sereno, T. J. Jr., and S. R. Bratt (1989). Seismic detection capability at NORESS and implications for the detection threshold of a hypothetical network in the Soviet Union, *J. Geophys. Res.* **94,** no. B8, 10,397–10,414.

Shi, Y., and B. A. Bolt (1982). The standard error of the magnitude-frequency b value, *Bull. Seism. Soc. Am.* **72,** 1677–1687.

Taylor, D. A., J. A. Snoke, I. S. Sacks, T. Takanami (1990). Nonlinear frequency magnitude relationship for the Hokkaido corner, Japan, *Bull. Seism. Soc. Am.* **80,** 340–353.

Utsu, T. (1965). A method for determining the value of b in a formula log n = a − bM showing the magnitude frequency for earthquakes, *Geophys. Bull. Hokkaido Univ.* **13,** 99–103.

Utsu, T. (1992). On seismicity, In *Report of the Joint Research Institute for Statistical Mathematics,* Institute for Statistical Mathematics, Tokyo, pp. 139–157.

Utsu, T. (1999). Representation and analysis of the earthquake size distribution: a historical review and some new approaches, *Pure Appl Geophys* **155,** 471–507.

Volant, P., and O. Scotti (1998). Deviations from self-organized critical state: a case study in the Western Alps, *EOS, Trans. Am. Geophys. Union,* F648.

Wiemer, S. Stefan Wiemer's Home Page, *http://www.seismo.ethz.ch/staff/stefan*

Wiemer, S., and M. Baer (2000). Mapping and removing quarry blast events from seismicity catalogs, *Bull. Seism. Soc. Am.* **90,** 525–530.

Wiemer, S., and J. Benoit (1996). Mapping the b-value anomaly at 100 km depth in the Alaska and New Zealand subduction zones, *Geophys. Res. Lett.* **23,** 1557–1560.

Wiemer, S., and K. Katsumata (1999). Spatial variability of seismicity parameters in aftershock zones, *J. Geophys. Res.* **103,** 13,135–13,151.

Wiemer, S., and S. McNutt (1997). Variations in frequency-magnitude distribution with depth in two volcanic areas: Mount St. Helens, Washington, and Mt. Spurr, Alaska, *Geophys. Res. Lett.* **24,** 189–192.

Wiemer, S., and M. Wyss (1997). Mapping the frequency-magnitude distribution in asperities: An improved technique to calculate recurrence times? *J. Geophys. Res.* **102,** 15,115–15,128.

Wiemer, S., S. R. McNutt, and M. Wyss (1998). Temporal and three-dimensional spatial analysis of the frequency-magnitude distribution near Long Valley caldera, California, *Geophys. J. Int.* **134,** 409–421.

Wyss, M., and A. H. Martyrosian (1998). Seismic quiescence before the M 7, 1988, Spitak earthquake, Armentia, *Geophys. J. Int.* **124,** 329–340.

Wyss, M., A. Hasegawa, S. Wiemer, and N. Umino (1999). Quantitative mapping of precursory seismic quiescence before the 1989, M 7.1, off-Sanriku earthquake, Japan, *Annali di Geophysica* **42,** 851–869.

Wyss, M., D. Schorlemmer, and S. Wiemer (2000). Mapping asperities by minima of local recurrence time: The San Jacinto-Elsinore fault zones, *J. Geophys. Res.* **105,** 7829–7844.

Zuniga, F. R., and S. Wiemer (1999). Seismicity patterns: are they always related to natural causes? *Pure Appl. Geophys.* **155,** 713–726.

Zuniga, R., and M. Wyss (1995). Inadvertent changes in magnitude reported in earthquake catalogs: Influence on b-value estimates, *Bull. Seism. Soc. Am.* **85,** 1858–1866.

Institute of Geophysics
ETH Hoenggerberg
CH-8093, Zurich, Switzerland
stefan@seismo.ifg.ethz.ch.
(S. W.)

Geophysical Institute
University of Alaska
Fairbanks, Alaska 99775
max@giseis.alaska.edu
(M. W.)

Manuscript received 12 August 1999.